EAI Endorsed Transactions
on Tourism, Technology and Intelligence
Research Article EAI.EU

Simultaneous Dual-Band Classification for WLAN Band Selection

Nana Esi Nyarko[1] and Quang N. Le[1]

[1]Memorial University, Canada

Abstract

Accurate classification of dual-band Wi-Fi signals is essential for improving adaptive band selection and maintaining quality of service in complex indoor wireless environments. Although several efforts have addressed propagation modeling, only few works simultaneously examined dual-band classification across both 2.4 GHz and 5 GHz frequencies in realistic scenarios. In this work, we use the measurements data conducted in the Deutsches Museum Bonn, which captures both line-of-sight (LoS) and non-LoS (NLoS) propagation conditions in a complex indoor environment. Ten statistical features are extracted from the received signal data, including mean, standard deviation, and skewness. To classify the signals, multiple machine learning models are evaluated, including k-nearest neighbors, support vector machines, and two deep learning architectures. Among these, model 3A, which is a fully connected neural network comprising three hidden layers using ReLU activation with 64, 32, and 16 neurons, respectively, and a softmax output layer, achieves the best performance. Trained with the Adam optimizer and categorical cross-entropy loss, model 3A attains an overall classification accuracy of 93 % at the optimal window, thus outperforming the baseline models in terms of precision, recall, and F1-score across all classes. These results highlight the model's robustness for simultaneous dual-band classification and its potential application in intelligent band selection for next generation Wi-Fi systems.

Received on 19 September 2025; accepted on 18 November 2025; published on 20 November 2025

Keywords: Dual-band Wi-Fi, machine learning, signal classification, WLAN

doi:10.4108/eettti.10327

1. Introduction

The field of wireless communication is on a groundbreaking transformation with the introduction and development of sixth-generation (6G) technology. This upcoming network aims to provide high data rates, ultra-low latency, and reliable connectivity, thus allowing a wide range of advanced applications, including independent systems and real-time remote operations [1]. Wi-Fi technologies, which include the new standards such as Wi-Fi 6 and 6E and new developments such as Wi-Fi 7, are expected to improve and support 6G networks [2]. As 6G aspires to create an insightful and interconnected digital ecosystem, there is a need for network speed, reliability, and the convergence of different communication technologies. The next generation Wi-Fi is going to play an important role in increasing localized high-speed connectivity, which will enable artificial intelligence (AI)-driven network optimization and support upcoming digital applications. One basic advantage of the next generation Wi-Fi is its ability to increase the speed of connectivity. Unlike cellular networks which require massive infrastructure, Wi-Fi is mostly installed indoors and provides cost-effective high-bandwidth communication [3]. Another key feature of the next generation Wi-Fi is its connection with AI-powered networks. Future networks will take advantage of the availability of AI and machine learning (ML) to improve network performance, spectrum allocation, and traffic management in real time. This will create a more stable connection that is free from interference, especially in concentrated urban and industrial settings [4].

The next generation Wi-Fi market is set to expand due to the rapid increase in consumers' demand for ultra-low, low-latency, and high-speed wireless

*Corresponding author. Email: nenyarko@mun.ca

connections. The principal force of this market growth is due to the growing digital ecosystem. The global Wi-Fi market is estimated to experience significant growth, which is fueled by technological innovation and business implementation of high-speed wireless networks. By 2030, more than 50 billion digital devices will be in operation, many of which will sorely rely on Wi-Fi connectivity for data exchange, remote management, and automation [5]. Wi-Fi will serve as a facilitator of smart city applications that include traffic management, AI-powered security surveillance, and energy-efficient grid networks. Similarly, next generation Wi-Fi will control innovations in industrial settings. In manufacturing and its logistics, the incorporation of Wi-Fi based automation will make real-time robotic control, AI-driven quality assurance, and predictive maintenance easier. This will result in reduced operational costs and increased productivity by taking advantage of industry 4.0 and industry 5.0 technologies. Looking at the entertainment sector, there will be a significant impact by next generation Wi-Fi especially in the area of gaming, cloud-based content streaming, and virtual collaboration. As extended reality (XR) technologies become mainstream, there will be an increase in demand for ultra-fast, cost-efficient Wi-Fi connectivity. Surpassing consumer uses, Wi-Fi development will reshape healthcare services, especially in telemedicine, AI-assisted diagnostics, and remote patient monitoring. With the growing need for real-time medical imaging and AI-driven healthcare solutions, hospitals and research centers will rely on high-speed Wi-Fi networks to facilitate wireless medical imaging, AI-assisted surgery, and digital health records management [6].

The next generation Wi-Fi symbolizes a major shift in wireless communications engineered to compliment 6G networks by providing high speed, cost-effective, and multiband connection to a wide range of applications. Its ability to operate across multiple frequency bands, from sub-6 GHz to millimeter-wave and terahertz spectrums, makes it necessary for next generation communication. However, achieving this vision presents several challenges, such as hardware limitations, network congestion, interference management, and energy efficiency [7]. A basic idea in wireless communication is the distinction between line-of-sight (LoS) and non-LoS (NLoS) propagation. LoS occurs when the path between the receiver and transmitter has no obstructions, whereas NLoS occurs when obstacles such as buildings, forest or vegetation, or walls obstruct this path, thus resulting in signal reflection, diffraction, or scattering [8]. This variation is very important, as it affects signal strength, quality, and overall network performance. In Wi-Fi systems, managing LoS and NLoS effectively is very essential to increase data transmission and ensure consistent connectivity, especially in a highly concentrated and complex environment [9]. With the use of dual-band systems that work over different frequencies, there has been an improvement in Wi-Fi over time. This has aided in making Wi-Fi connections more reliable indoors. Dual-band Wi-Fi allows devices to connect to two different frequency bands, thus giving more options to balance coverage, speed, and signal strength. The 2.4 GHz band signal can travel through walls and obstacles better, whilst the 5 GHz band allows for faster internet speeds when there are fewer barriers [10]. The performance of wireless communication is highly dependent on how signals travel between access points and receivers [11]. Recognizing and differentiating between NLoS and LoS paths is necessary for the improvement of indoor wireless connections. Each frequency band exhibits distinct propagation characteristics. In contrast, 2.4 GHz signals typically propagate further and penetrate obstacles more effectively, though with lower achievable data rates [10]. To address how these frequency bands behave in changing indoors settings, dual band systems employ LoS and NLoS classification. This creates better signal models and allows the system to select the best frequency based on real-time conditions.

There are several benefits that using dual-band classifications can bring, such as good signal prediction and quality network performance by choosing the best frequency. LoS and NLoS signal paths make it difficult to keep wireless connections reliable, especially in Wi-Fi's. New Wi-Fi technologies incorporate modern or progressive features, which include beamforming, multiple-input multiple-output systems, and high-order modulation schemes, to increase signal quality and decrease the negative effect of NLoS propagation. Accurate channel estimation plays an important role in these systems by adjusting signal settings, improving direction control, and allowing multiple connections at once. Dual-band Wi-Fi technologies make it even more challenging to handle both LoS and NLoS signal propagation by analyzing the signal behavior across multiple frequency bands; systems can more accurately identify propagation conditions, thus allowing better decision-making for routing and resource allocation [12]. Furthermore, recognizing the propagation environment aids in dynamic adjustments, such as changing frequency bands or transmission power, to maintain the best performance [13]. The best band selection strategies can increase network performance, reduce delays, and make the overall user experience better. However, the dynamic and unpredictable nature of wireless environments characterized by multipath fading, interference, and fluctuating signal strength makes it difficult to consistently select the optimal frequency band. These challenges have been addressed through various adaptive band selection and ML techniques,

such as reinforcement learning and neural network-based classifiers, which can learn from real-time channel conditions to predict the best band. While such techniques improve adaptability, they also increase computational complexity and require large datasets for accurate model training.

This paper aims to investigate the concept of simultaneous dual-band classification for Wi-Fi band selection and emphasize innovative approaches that enable efficient decision-making in real-time network environments. While previous studies have applied ML algorithms for band prediction and selection, most have focused on single-band optimization or simplified propagation models. In contrast, this work introduces a simultaneous dual-band classification framework using ray tracing-derived datasets, designed to handle realistic indoor propagation effects. This has the potential to enhance wireless communications, minimize interference, and improve overall network performance, which is crucial as the demand for high-speed wireless connectivity steadily increases.

2. Background

Wireless communication systems have evolved to meet the growing demand for high-speed data transmission, efficient spectrum usage, and robust connectivity. The IEEE 802.11 standards for wireless local area networks (WLANs) assist 2.4 GHz and 5 GHz activities. Industrial, scientific, and medical bands are instrumental in wireless infrastructures. The 2.4 GHz band offers exceptional circulation features as a result of its lower frequency, whilst as a result of separate channel availability, the 5 GHz provides higher bandwidth with little interference [14]. Dual-band WLAN utilizes these features, but they only run smoothly if bands are chosen thoughtfully and adjusted dynamically. To obtain an ideal performance, there is a need to identify and improve both frequency bands simultaneously. This aids in providing great quality of service, reducing interference, and assisting in the flexible management of resources in different environments [15]. In reference to [15], a research on comparing Wi-Fi documentation and signal profiling methods in both frequency bands, with a focus on location precision and power usage, was conducted. The results of this study revealed that the 5 GHz band offers higher data rates and, as a result, uses more energy, whilst the 2.4 GHz band is more power-efficient. The findings from this study reveal the need to balance energy consumption and data speed. This can be achieved through an adaptive dual-band selection mechanism. Also, ray tracing simulations were used to analyze signal behavior in confined spaces such as aircraft cabins. The results showed that environmental factors such as passenger movement and structural obstacles reduce signal quality significantly, especially at higher frequencies. Also, to optimize WLAN performance, band selection algorithms must consider the surrounding environment. Further analysis in [3] addressed the complexities of resource allocation in multi-band communication systems, particularly 5 GHz and sub-6 GHz coexistence. The research highlighted and focused on key challenges such as inter-band interference, latency introduced by concurrent operations, and sub-optimal spectrum utilization. Simultaneous classification approaches such as multi-band convolutional neural networks and ensemble learning models have been proposed to enhance spectrum efficiency and reduce cross-band contention by jointly analyzing signal features from both 2.4 GHz and 5 GHz channels for optimal band allocation. Their conclusions emphasized the need for strong decision-making frameworks in order to manage the dynamic spectrum conditions. Beyond WLANs, precise indoor localization remains a critical area, particularly for mission-critical applications requiring sub-meter precision. Ultra-wideband (UWB) systems offer high temporal time resolution for accurate distance measurements. However, UWB performance is very sensitive to signal reflections, i.e., multipath propagation, and signal obstructions [16]. As detailed, distinguishing between LoS and NLoS signal components is key to minimizing positioning errors. NLoS paths introduce extra delay, which is caused by reflections and diffractions; this reduces accuracy, unless they are properly identified and filtered out. This implies that reliable UWB localization requires pre-processing techniques to isolate direct paths from obstructed paths, using signal features like time-of-arrival and received signal strength (RSS) indicator variations. The increase in data-intensive applications like real-time streaming and mobile internet has driven the shift from narrowband to broadband access, with technologies evolving from GSM/EDGE to more efficient 5G/5G-A systems for better speed and efficiency. Cognitive radio (CR) represents a revolution in wireless technology by enabling systems to dynamically access the smart spectrum, thus adapting to the environment and coordinating with other networks. However, practical deployment of CR faces significant hurdles like reliable spectrum sensing, real-time interference avoidance, and regulations, thus requiring advanced AI-based control and integrated protocols [14]. Moving into the future, the performance and scalability of wireless systems depend on tackling several critical challenges. These include: (1) Implementing smart congestion control mechanisms to manage network density and increased traffic loads, (2) developing precise channel models that capture the intricacies of signal propagation in dense and dynamic environments, (3)

developing energy-efficient protocol stacks to prolong battery life in devices with limited power. Furthermore, improved handling of LoS and NLoS signal effects and the diverse nature of the spectrum will be crucial for maintaining signal integrity and reducing interference between systems. Addressing these issues will be vital for maximizing the efficiency and user-friendliness of future wireless ecosystems.

3. Dataset and Feature Engineering

The dataset utilized in this study originates from the work presented in [10], which conducted extensive dual-band measurements within two representative indoor environments: the Deutsches Museum Bonn (DMB) and the ICT Cubes at RWTH Aachen University. The experimental setup involved two omnidirectional transmission antennas operating at 2.4 GHz and 5 GHz, specifically designed to ensure uniform radiation across the azimuthal plane. This configuration enabled a comprehensive evaluation of frequency-dependent propagation characteristics under real-world conditions. Vertical gain patterns were employed to assess elevation-dependent performance and identify potential directional attenuation. The combined analysis facilitated a systematic comparison between the two frequency bands, thus revealing critical differences in signal behavior across environments and informing strategies for enhancing WLAN performance and robustness in complex indoor scenarios. Measurements were taken at the two frequencies, 2.4 GHz and 5 GHz, respectively. Multiple measurement routes were followed for each environment, with a careful definition of the transmitter and receiver positions. The measurements were recorded using specialized equipment capable of averaging multiple readings per point to minimize small-scale fading. The data includes RSS values under both LoS and NLoS conditions. The datasets accounted for the antenna's characteristics. The feature engineering in this paper takes raw measurement data and turns it into useful input for modeling and analysis. This process involves preprocessing the data and then calculating important statistical metrics and derived features such as mean, standard deviation, maximum. These features capture the essential characteristics of the signals, thus allowing for strong classification and predictive modeling. To transform the raw simulation output into a format suitable for ML as shown in figure 1, significant statistical and signal features were obtained from different parts of the received power data. Let P_i denote the received power of the i-th sample in a given window of N measurements. The extracted features include mean, standard deviation (SD), skewness (SK), kurtosis (KT), half skewness (hSK), max, min, distribution ratio (D-Ratio), geometric mean (Gmean), and range. The variables and equations used in the feature extraction process are shown as follows:

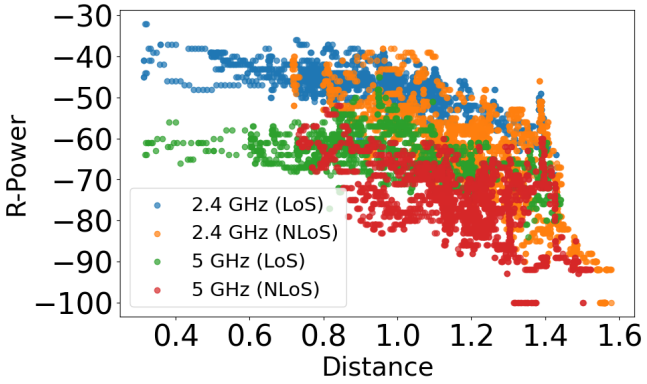

Figure 1. A visualization of feature of R-power to aid in and pattern recognition.

- **Mean (μ):** It is the average signal power within the window, as shown in figure 2. The higher the mean, the stronger the signal regions. This helps to separate bands with different attenuation behavior. μ is calculated as follows:

$$\mu = \frac{1}{N}\sum_{i=1}^{N} P_i. \tag{1}$$

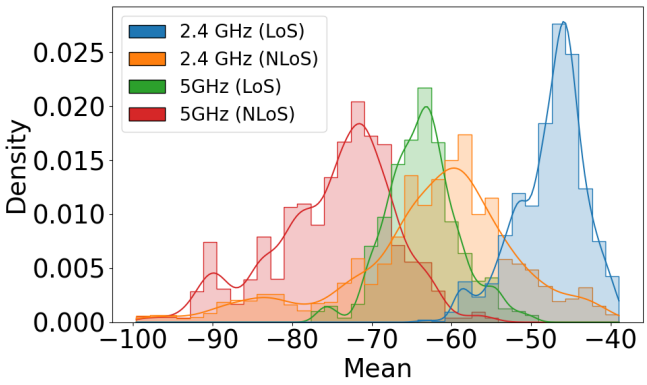

Figure 2. A feature distribution of Mean.

- **SD (σ):** The spread or variability of signal power. It quantifies how much the power fluctuates. This helps to capture multipath fading intensity, which varies between 2.4 GHz and 5 GHz due to propagation differences. σ is given by

$$\sigma = \sqrt{\frac{1}{N}\sum_{i=1}^{N}(P_i - \mu)^2}. \tag{2}$$

- **SK:** It measures asymmetry of the power distribution and identifies bias in fading behavior. For instance, whether most of the signal values are clustered below or above the mean. Different bands may exhibit different SK due to interference or blockage. SK is shown as

$$SK = \frac{1}{N}\sum_{i=1}^{N}\left(\frac{P_i - \mu}{\sigma}\right)^3. \tag{3}$$

- **KT:** It measures "tailedness" or extremity of power values. This helps to detect outliers and rare strong/weak signal spikes. High KT may indicate sporadic interference or dominant line-of-sight paths. KT is derived as

$$KT = \frac{1}{N}\sum_{i=1}^{N}\left(\frac{P_i - \mu}{\sigma}\right)^4. \tag{4}$$

- **hSK:** Derived from higher statistical moments, this feature enhances sensitivity to subtle changes in signal asymmetry. It can capture non-obvious signal shape properties that lower-order moments miss, thus improving classification robustness. This phenomenon is shown in figure 3.

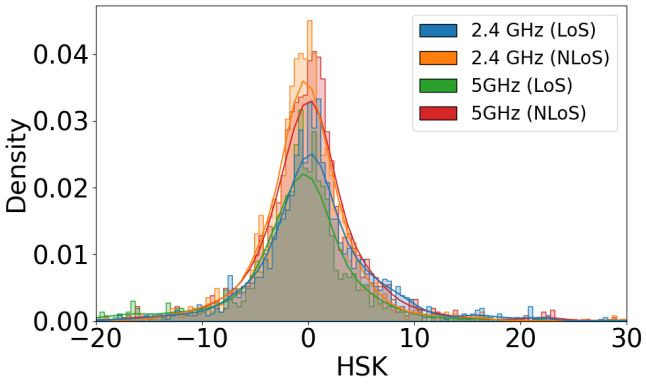

Figure 3. A feature distribuution of HSK.

- **Max:** It indicates the strongest received signal in a window, which is useful for identifying direct LoS dominance or reflective boosts. Max is given by

$$\max(P_i). \tag{5}$$

- **Min:** It highlights shadowed or obstructed signal regions. When combined with max, it reveals signal spread. Min is written as

$$\min(P_i). \tag{6}$$

- **Range:** It captures the overall variability in signal strength. A high dynamic range often signals more complex multipath or interference patterns. It is calculated as

$$\text{Range} = \max(P_i) - \min(P_i). \tag{7}$$

- **Gmean:** It provides a multiplicative average that is less sensitive to extreme values, thus offering a complementary view to the arithmetic mean. Gmean is derived as

$$\text{Gmean} = \left(\prod_{i=1}^{N} P_i\right)^{1/N}. \tag{8}$$

- **D-Ratio:** It normalizes variability by average power. High D-Ratio may indicate unstable channels, which is useful for distinguishing high-fading versus stable environments across bands. D-Ratio is given by

$$\text{D-Ratio} = \frac{\sigma}{\mu}. \tag{9}$$

4. Proposed Model, Training, and Testing Approach

For classification of wireless signals based on the features which are derived from the indoor measurements, a ML framework is proposed. At 2.4 GHz and 5 GHz, signals turn to face interference. Therefore, a reliable model is needed to accurately classify the frequency bands. A supervised learning method based on an artificial neural network architecture, configured as a feedforward multilayer perceptron, is implemented to resolve this. The input layer accepts ten features extracted from the measurement data. These features describe overall patterns and complex variations in signal strength, thus aiding in distinguishing between different frequency bands. The hidden layers utilize a rectified linear unit (ReLU) activation function. The final output layer uses a softmax activation function across the four classes, i.e., 2.4 GHz LoS, 2.4 GHz NLoS, 5 GHz LoS, and 5 GHz NLoS, to enable multiclass probability estimation for band classification. Data preprocessing is essential for the model to work well. First, the dataset is split into input features that help to make predictions, and class labels that show the correct answers. Feature scaling is performed using standardization. The dataset is divided into two parts: 80% for training the model and 20% for testing it. The test data are kept separately during training to ensure that the evaluation is fair and unbiased. During training, the model adjusts its settings repeatedly to reduce error between the predicted probabilities and the true class labels. After each epoch, the training progress is monitored and the final settings are chosen based

on the full training period, without stopping early. As described above, figure 4 presents the workflow for data preprocessing, model training, and evaluation in dual-band classification.

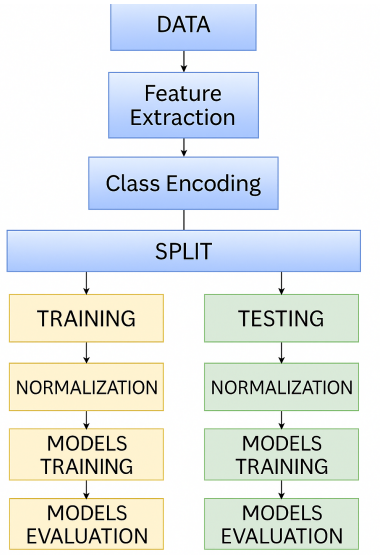

Figure 4. Workflow of data preprocessing, model training, and evaluation for dual-band classification.

The core of the model, labeled as model 3A, comprises three hidden layers. The first hidden layer is made up of 64 neurons, followed by a second layer with 32 neurons and a third layer with 16 neurons. A second architecture labeled as model 3B is a control model, which uses the same input and output set-up but has only two hidden layers: The first with 64 neurons, and the second with 32 neurons. All layers utilize the ReLU activation function. The performance of the model is evaluated by using Loss function, which is calculated as follows:

$$\mathcal{L} = -\sum_{i=1}^{N}\sum_{c=1}^{C} y_{ic}\log(\hat{y}_{ic}), \tag{10}$$

where N is the number of samples, C is the number of classes, y_{ic} is the binary indicator (0 or 1) if class label c is the correct classification for sample i, and $\hat{y}_{ic}$ is the predicted probability that sample i is of class c.

- **Precision:** It measures the proportion of correctly predicted positive instances among all predicted positives, which is shown as

$$\mathrm{P} = \frac{TP}{TP + FP}, \tag{11}$$

where

  - TP = True Positives (correctly predicted positive instances)
  - FP = False Positives (incorrectly predicted positive instances)

- **Recall (Sensitivity/True positive rate):** It measures the proportion of correctly predicted positives among all actual positives, which is given by

$$\mathrm{R} = \frac{TP}{TP + FN}, \tag{12}$$

where

  - FN = False Negatives (actual positives incorrectly predicted as negatives)

- **F1-Score:** It is the harmonic mean of Precision and Recall, which emphasizes the balance between the two metrics. It is derived as

$$\mathrm{F}_1 = \frac{2 \times (\mathrm{P} \times \mathrm{R})}{\mathrm{P} + \mathrm{R}}, \tag{13}$$

where

  - P = Precision
  - R = Recall

- **Accuracy:** It is the proportion of correctly predicted instances (both positive and negative) out of the total instances, which is given by

$$\mathrm{A} = \frac{TP + TN}{TP + TN + FP + FN}, \tag{14}$$

where

  - TN = True Negatives (correctly predicted negative instances)

- **Macro Average:** It calculates the metric independently for each class and then takes the mean, which is shown as

$$\mathrm{M}_A = \frac{1}{N}\sum_{i=1}^{N} m_i, \tag{15}$$

where

  - N = Number of classes
  - m_i = Metric value for the i-th class

- **Weighted Average:** It accounts for the support of each class, which makes it more representative for imbalanced data. It is calculated as follows:

$$\mathrm{W}_A = \frac{\sum_{i=1}^{N}(s_i \times m_i)}{\sum_{i=1}^{N} s_i}, \tag{16}$$

where

– s_i = Support for the i-th class (number of instances)

Support vector machine (SVM) and k-nearest neighbors (KNN) are used as control models, which provide the benchmark performance metric. They serve as reference points, which provide a detailed evaluation of the classification accuracy and window size parameters.

5. Simulation Results and Discussions

This section shows the results of conducted simulations, which aided in evaluating the performance of the proposed models. We aim to distinguish between the effectiveness of the model's classification against standard benchmarks, i.e., SVM and KNN, and deriving meaningful insights from the analysis. The used models are evaluated based on their ability to differentiate and classify specific signal bands, i.e., 2.4 GHz and 5 GHz, under different conditions such as LoS and NLoS.

5.1. Performance of the Proposed Model over All Windows

Based on its outstanding classification accuracy during preliminary testing, model 3A is selected as the proposed model for this study. This section presents a detailed evaluation of its performance across windows. The analysis of model 3A is conducted over a series of windows ranging from window 10 to window 35. This is done to determine how the different windows affect the classification performance and to also identify the best configuration for accurate band selection in dual-band Wi-Fi selection. As shown in figure 5, model 3A shows a strong and consistent improvement in accuracy as the window size increases. Beginning with an accuracy of 82.42% in window 10, the model rises to 88.39% in window 12. From window 13 to 18, there is a stabilization in the accuracy, ranging from 87% to 89%. This suggests that there is a brief saturation in performance gains irrespective of the increasing input size. There is a notable boost in the performance around window 20 with an accuracy of 90%. This pattern continues with minor fluctuations, by window 22 the model reaches a stable accuracy of 93%. From window 23 onwards, the model reaches a stable phase of strong performance where the accuracy remain consistently strong through subsequent windows ranging between 94% and 96%. While various windows show the model's full learning potential, the accuracies beyond window 22 become irrelevant. Practically, windows 22 offers an ideal balance between data processing and accuracy in data categorization as the performance curve begins to plateau. Although marginal improvement continues beyond window 22, the accuracy becomes less significant compared to the extra computing cost. This makes window 22 is well-suited for dual-band Wi-Fi classification.

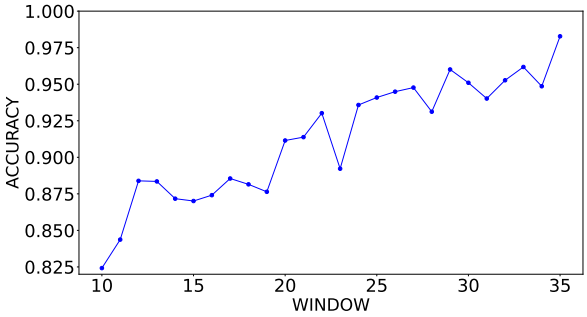

Figure 5. Accuracy of the proposed model 3A across different windows.

5.2. Performance of Different Features on the Proposed Model

An additional evaluation is conducted to investigate how the integration of different features affects the classification performance of the proposed model, i.e., model 3A. Table 1 shows ten sets of feature labeled from A to J are examined to analyze the contribution of each feature to the overall model accuracy. The features are progressively inceased and labeled from A to J. Each label represents a cumulative set of features used for the training model 3A.

Table 1. Cumulative feature combinations and their correspond labels.

Cumulative Features	Label
Mean	A
Mean, SD	B
Mean, SD, SK	C
Mean, SD, SK, KT	D
Mean, SD, SK, KT, hSK	E
Mean, SD, SK, KT, hSK, Max	F
Mean, SD, SK, KT, hSK, Max, Min	G
Mean, SD, SK, KT, hSK, Max, Min, D-Ratio	H
Mean, SD, SK, KT, hSK, Max, Min, D-Ratio, Gmean	I
Mean, SD, SK, KT, hSK, Max, Min, D-Ratio, Gmean, Range	J

As shown in figure 6, the model shows a steady increment in the performance of the features as they are cumulatively increased. This pattern reflects how detailed the input becomes, which helps the model to capture the characteristics of the signal. By the time the cumulative increment of the features reaches G, the accuracy surpasses 90%, which shows a significant performance gain. Further increments,

such as including D-Ratio in feature H, Gmean in feature I, and Range in feature J, yield incremental improvements, with feature J achieving the highest accuracy of nearly 98%. These results show the effect of combining different features. Each added feature helps the model better understand Wi-Fi signals and improves accuracy. However, after a certain point, the extra features don't add much benefit, which indicates that excessive complexity doesn't always lead to better performance.

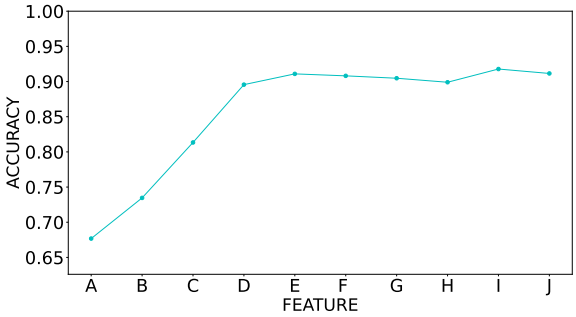

Figure 6. Feature accumulation accuracy of model 3A.

5.3. Comparison with Other Models and Computational/Complexity Analysis

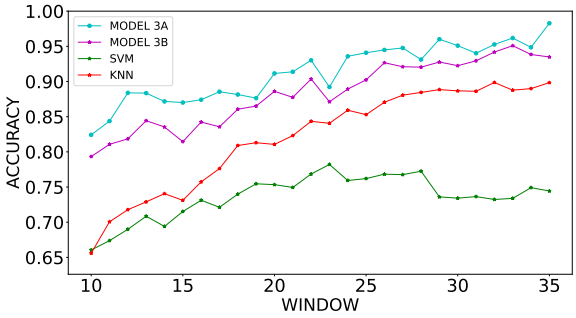

Figure 7. Windows accuracy comparison of models classification.

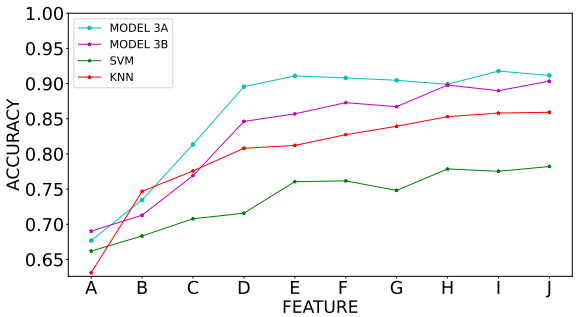

Figure 8. Feature accuracy comparison of models classification.

The analysis of model 3A against baseline models, i.e., model 3B, KNN, and SVM, is carried out using two approaches: feature-based performance (A–J) and window-based accuracy (window from 10 to 35). The aim is to assess both the classification accuracy and computational efficiency, which are very important for real-time dual-band classification in wireless environments. In terms of classification performance as indicated in figure 7, model 3A demonstrates a higher classification compared to other models. This analysis highlights model 3A's reliability. From an accuracy of 83% at window 10, there is a consistent improvement of the model as it peaks at 98% by window 35. Model 3B follows a similar upward trend but remains about 2% lower on average. KNN and SVM also show a notable increase, achieving 90% and 75%, respectively, at their best.

In figure 8, model 3A shows rapid progress from 67% accuracy with feature A to over 91% with feature J. The performance of the model increases as more features are included, which indicates that the use of statistical features together greatly improves the learning capability of the model. Model 3B, while similar to 3A, stabilizes at a slightly lower accuracy of around 90%. In contrast, KNN and SVM present a more modest improvement, with the accuracy of KNN reaching about 86% at the J feature set while SVM plateaus around 78%, thus showing less responsiveness to feature increments.

Beyond accuracy, computational efficiency is an important factor when it comes to the selection of a model for real-time systems. Table 2 compares the models in terms of complexity, efficiency, and scalabity. Model 3A, which is a neural network with 3 hidden layers, requires moderate to high computational resources during training. Some of the computing load is reduced with the use of ReLU activation and Adam optimizer. Once trained, model 3A is highly efficient. With model 3B being similar in architecture but less complex, it benefits from model 3A's efficiency but doesn't match the accuracy. Its computational demands are moderately lower during training as a result of few layers. In contrast, KNN has a lower computational requirement during training but becomes computationally expensive during inference. During prediction, KNN requires the calculation of distances from the test point to every training sample. As the dataset grows, the performance of the model decreases. This makes KNN less suitable for real-time classification tasks, especially when the input data volume is high. SVM also presents computational challenges, particularly with non-linear kernels like radial basis function (RBF). Its complexity during training increases as the dataset also grows, thus increasing its computational requirements. Additionally, SVM's reliance on support vectors for

Table 2. Computational complexity and performance comparison of Model 3A, Model 3B, KNN, and SVM.

Model	Training Complexity	Inference Complexity	Efficiency	Scalability
Model 3A	Moderate (Deep learning)	Low (Efficient after training)	High (GPU optimized)	High (Deep learning)
Model 3B	Moderate (Fewer layers)	Low (Efficient after training)	High	Good
KNN	Low (Data storage only)	High (Distance calculation)	Low (Inefficient at scale)	Poor (Memory-intensive)
SVM	High (Kernel complexity)	Moderate (Support vectors)	Moderate	Limited (Non-linear data)

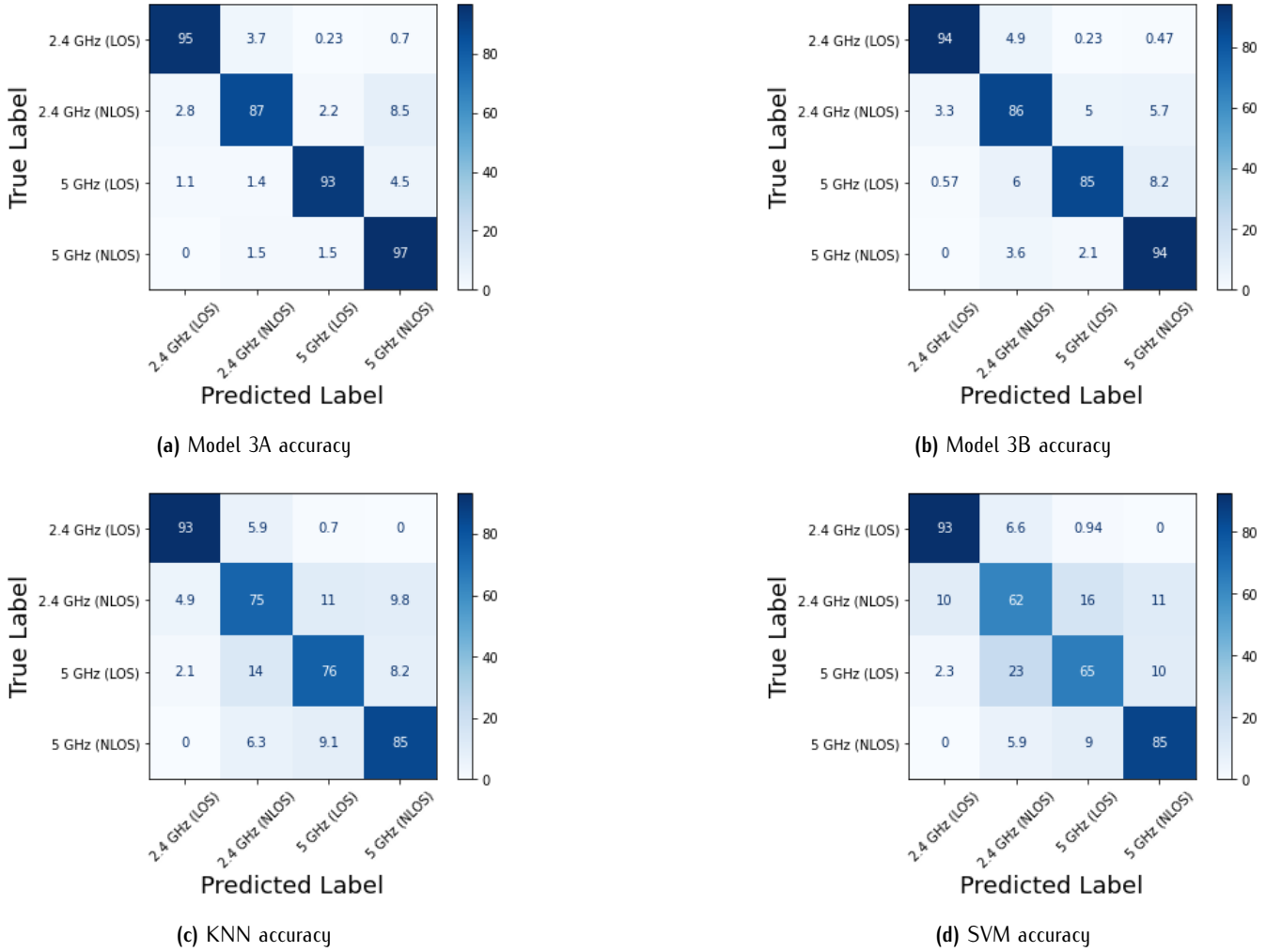

(a) Model 3A accuracy

(b) Model 3B accuracy

(c) KNN accuracy

(d) SVM accuracy

Figure 9. Comparison of accuracy metrics for different models.

its predictions makes it slower during prediction compared to pre-trained neural networks.

In addition to evaluating the accuracy and computational efficiency of the models, confusion matrices are illustrated in figure 9. Also, a comparative analysis of classification reports, which is shown in table 3, provide deeper insights into the different models' performance across different classes. Among all the models, model 3A demonstrates the most robust classification performance, with consistently high scores across all classes. The precision and recall values indicate balanced and accurate classification for both LoS and NLoS conditions at 2.4 GHz and 5 GHz. Model 3B also exhibits high accuracy, reaching 90% overall. However, it consistently performs slightly lower than model 3A in all categories. KNN, which is a simpler model compared to neural networks, achieves an accuracy of 82%. The confusion matrix reveals that while KNN performs well in detecting 2.4 GHz LoS, its performance significantly drops for 2.4 GHz NLoS and 5 GHz LoS. The 5 GHz NLoS class shows a reasonable balance, but overall, the model's accuracy and recall are notably lower than the neural network models. SVM, which uses the RBF kernel, achieves the lowest accuracy among the compared models at 77%. The confusion matrix highlights

Table 3. Performance comparison of classification models.

Class/Metric	Model 3A (%)	Model 3B (%)	KNN (%)	SVM (%)
2.4 GHz LoS	Precision: 96.0 Recall: 95.0 F1-Score: 96.0	Precision: 96.0 Recall: 94.0 F1-Score: 95.0	Precision: 93.1 Recall: 94.9 F1-Score: 94.0	Precision: 91.0 Recall: 94.0 F1-Score: 93.0
2.4 GHz NLoS	Precision: 93.0 Recall: 87.0 F1-Score: 90.0	Precision: 87.0 Recall: 86.0 F1-Score: 86.0	Precision: 73.1 Recall: 79.0 F1-Score: 76.0	Precision: 77.0 Recall: 79.0 F1-Score: 78.0
5 GHz LoS	Precision: 95.0 Recall: 93.0 F1-Score: 94.0	Precision: 90.0 Recall: 85.0 F1-Score: 87.0	Precision: 85.2 Recall: 75.8 F1-Score: 80.2	Precision: 79.0 Recall: 75.0 F1-Score: 77.0
5 GHz NLoS	Precision: 90.0 Recall: 97.0 F1-Score: 93.0	Precision: 90.0 Recall: 94.0 F1-Score: 92.0	Precision: 87.1 Recall: 88.0 F1-Score: 87.6	Precision: 88.0 Recall: 88.0 F1-Score: 88.0
Accuracy	93.0	90.0	84.4	84.0

significant challenges in correctly classifying 2.4 GHz NLoS and 5 GHz LoS.

6. Conclusion

This study explores different ML models for classifying dual-band Wi-Fi signals, including model 3A, model 3B, KNN, and SVM. Among them, the proposed model 3A achieves the highest accuracy and shows strong and balanced performance across both 2.4 GHz and 5 GHz bands, as well as in LoS and NLoS conditions. It consistently outperforms the other models in terms of precision, recall, and F1-score. The feature selection analysis shows that adding more features gradually improves classification performance, with the full feature set, i.e., label J, giving the best results. The confusion matrix and classification reports further confirm that model 3A can detect subtle signal differences that other models miss, especially in challenging NLoS cases. Although KNN and SVM are simpler, they lack the scalability and accuracy of model 3A. Overall, model 3A proves to be a reliable and efficient choice for dual-band signal classification, which supports smarter and more adaptive Wi-Fi band selection in complex indoor environments.

References

[1] Letaief KB, Shi Y, Lu J, Lu J. Edge Artificial Intelligence for 6G: Vision, Enabling Technologies, and Applications. IEEE Journal on Selected Areas in Communications. 2022 Jan;40(1):5-36.

[2] Rodrigues Dias Filgueiras H, Saia Lima E, Sêda Borsato Cunha M, De Souza Lopes CH, De Souza LC, Borges RM, et al. Wireless and Optical Convergent Access Technologies Toward 6G. IEEE Access. 2023;11:9232-59.

[3] Tataria H, Shafi M, Molisch AF, Dohler M, Sjöland H, Tufvesson F. 6G Wireless Systems: Vision, Requirements, Challenges, Insights, and Opportunities. Proceedings of the IEEE. 2021;109(7):1166-99.

[4] Saad W, Bennis M, Chen M. A Vision of 6G Wireless Systems: Applications, Trends, Technologies, and Open Research Problems. IEEE Network. 2020;34(3):134-42.

[5] Rangan S, Rappaport TS, Erkip E. Millimeter-Wave Cellular Wireless Networks: Potentials and Challenges. Proceedings of the IEEE. 2014;102(3):366-85.

[6] Srinivasu PN, Ijaz MF, Shafi J, Woźniak M, Sujatha R. 6G Driven Fast Computational Networking Framework for Healthcare Applications. IEEE Access. 2022;10:94235-48.

[7] Naik G, Park JM, Ashdown J, Lehr W. Next Generation Wi-Fi and 5G NR-U in the 6 GHz Bands: Opportunities and Challenges. IEEE Access. 2020;8:153027-56.

[8] Shi Y, Enami R, Wensowitch J, Camp J. Measurement-based characterization of LOS and NLOS drone-to-ground channels. In: 2018 IEEE Wireless Communications and Networking Conference (WCNC). Barcelona, Spain; 2018. p. 1-6.

[9] Sandoval O, David González G, Hämäläinen J, Yoo S. Indoor planning and optimization of LTE-U radio access over WiFi. In: 2016 IEEE 27th Annual International Symposium on Personal, Indoor, and Mobile Radio Communications (PIMRC). Valencia, Spain; 2016. p. 1-7.

[10] Preusser K, Schmeink A. Robust Channel Modeling of 2.4 GHz and 5 GHz Indoor Measurements: Empirical, Ray Tracing, and Artificial Neural Network Models. IEEE Transactions on Antennas and Propagation. 2022;70(1):559-72.

[11] Fahem Majeed A, Arsat R, Ariff Baharudin M, Mu'Azzah Abdul Latiff N, Albaidhani A. Accurate Multiclass NLOS Channels Identification in UWB Indoor Positioning System-Based Deep Neural Network. IEEE Access. 2024;12:179431-48.

[12] Zhang Z, Qingyang Hu R. Dense Cellular Network Analysis With LoS/NLoS Propagation and Bounded Path Loss Model. IEEE Communications Letters. 2018;22(11):2386-9.
[13] Huang L, Kumar S, Kuo CCJ. Adaptive resource allocation for multimedia QoS management in wireless networks. IEEE Transactions on Vehicular Technology. 2004;53(2):547-58.
[14] Duong D, Xu Y, David K. Comparing the Performance of Wi-Fi Fingerprinting Using the 2.4 GHz and 5 GHz Signals. In: 2018 IEEE 87th Vehicular Technology Conference (VTC Spring). Porto, Portugal; 2018. p. 1-5.
[15] Aboagye S, Amin Saeidi M, Tabassum H, Tayyar Y, Hossain E, Yang HC, et al. Multi-Band Wireless Communication Networks: Fundamentals, Challenges, and Resource Allocation. IEEE Transactions on Communications. 2024;72(7):4333-83.
[16] Pärssinen A. Multimode-multiband transceivers for next generation of wireless communications. In: 2011 Proceedings of the European Solid-State Device Research Conference (ESSDERC). Helsinki, Finland; 2011. p. 42-53.